Supporting Materials

Covalent Organic Polymer Supported Palladium Catalyst for CO Oxidation

You Zhou[†], Zhonghua Xiang[‡], Dapeng Cao[*,‡], and Chang-Jun Liu[*,†]

[†]School of Chemical Engineering and Technology, Tianjin University, Tianjin 300072, China

[‡]State Key Laboratory of Organic-Inorganic Composites, Beijing University of Chemical Technology, Beijing 100029, PR China

The supporting materials contain details of the catalyst characterization, reaction of CO oxidation, results of the catalysts obtained by hydrogen reduction, figures of the isotherms and HK pore size distribution, discussions with TGA analyses and TEM images of the catalysts (by electron reduction at room temperature) after reaction.

1. Characterization details

X-ray diffraction (XRD) and transmission electron microscopy (TEM) were used to estimate metal dispersion. The XRD patterns were recorded with a Rigaku D/MAX-2500 V/PC using Cu radiation (40 kV and 200 mA). The TEM observations were performed using a Philips TECNAI G^2F20 system.

N_2-physisorption for determining the specific surface area and pore size distribution were performed at liquid nitrogen temperature using an Autosorb-1 analyzer from Quantachrome Instruments (AUTOSORB-1-C). The samples were degassed at 150 ^oC for 6 h under vacuum before analysis. The Langmuir and BET methods were employed to calculate the specific surface areas. The pore size distributions were derived from the isotherms using the HK model.

Thermogravimetric Analysis (TGA) was performed to determine the thermal stability of the samples. It was carried out under a N_2 atmosphere (total flow: 30 mL/min) at a constant rate of 10 ^oC/min, using a Netzsch STA 449 F3 system.

The IR spectra were obtained on a BRUKE Tensor-27 spectrometer equipped with a diffuse reflectance accessory. For Diffuse reflectance Fourier transform infrared (DRIFT) spectra of adsorbed CO, the catalyst samples were purged by He (20 ml/min) at 150 °C for 1 h, then exposed to 20 mL/min CO (1.11 vol.%) / helium at 25 °C for 30 min. After the cell was flushed with He for another 30 min, the DRIFT spectra were recorded at a resolution of 4 cm^{-1} and 64 scans. For FT-IR spectra, 1.5 mg of the sample was mixed thoroughly with 200 mg of homogenized porcelain-milled KBr (FT-IR grade), and pressed into a wafer. Then the wafer was put into the sample holder and FT-IR spectra were recorded at a resolution of 4 cm^{-1} and 64 scans.

2. **Reaction**

The catalytic oxidation of CO was carried out in a quartz-tube (i.d. 4 mm) fixed-bed reactor. The catalyst (10 mg, powder) was pretreated at 300 ^oC in a flow of 20 ml/min argon for 1 h. After cooling to the room temperature, the mixture gas (total flow = 20 ml/min, 1.0 vol.% CO / 20 vol.% O_2 / balance N_2) was fed into the reactor . For each temperature point, there was duration of 40 min. The effluent was analyzed using an on-line gas chromatograph (Agilent 6890) equipped with a Porapak Q column and a thermal conductivity detector (TCD).

3. Results over the catalyst by hydrogen reduction at 300°C

Compared to the electron reduction via glow discharge at room temperature, the hydrogen reduction leads to a formation of larger particles, as shown in Figure S1. The particles of the Pd/COP-4-WH (W=Water, H= hydrogen reduction) sample are homo-dispersed on the layered support with similar size about 9.9 nm, as shown in Figure S1 (d. e. f.). By contrast, the Pd/COP-4-DH (D=DMF) sample had particles no larger than 5 nm, as well as some agglomeration with different sizes. The mean size is about 7.7 nm. Figure S1 (g. h. i.) obviously revealed the nonuniform of the particle size and dispersion. Some particles in the Pd/COP-4-WH sample showed distinct lattice fringes. As shown in Figure S1c, the lattice fringes with d = 0.224 nm could be attributed to the Pd(111) planes, which implied there was Pd^0 on the Pd/COP-4-WH sample. Comparing the images of the support before and after the loading of Pd species, we can find some change of the structure, which was more obvious for the Pd/COP-4-DH sample. The XRD results shown in Figure S2 confirmed the TEM analyses.

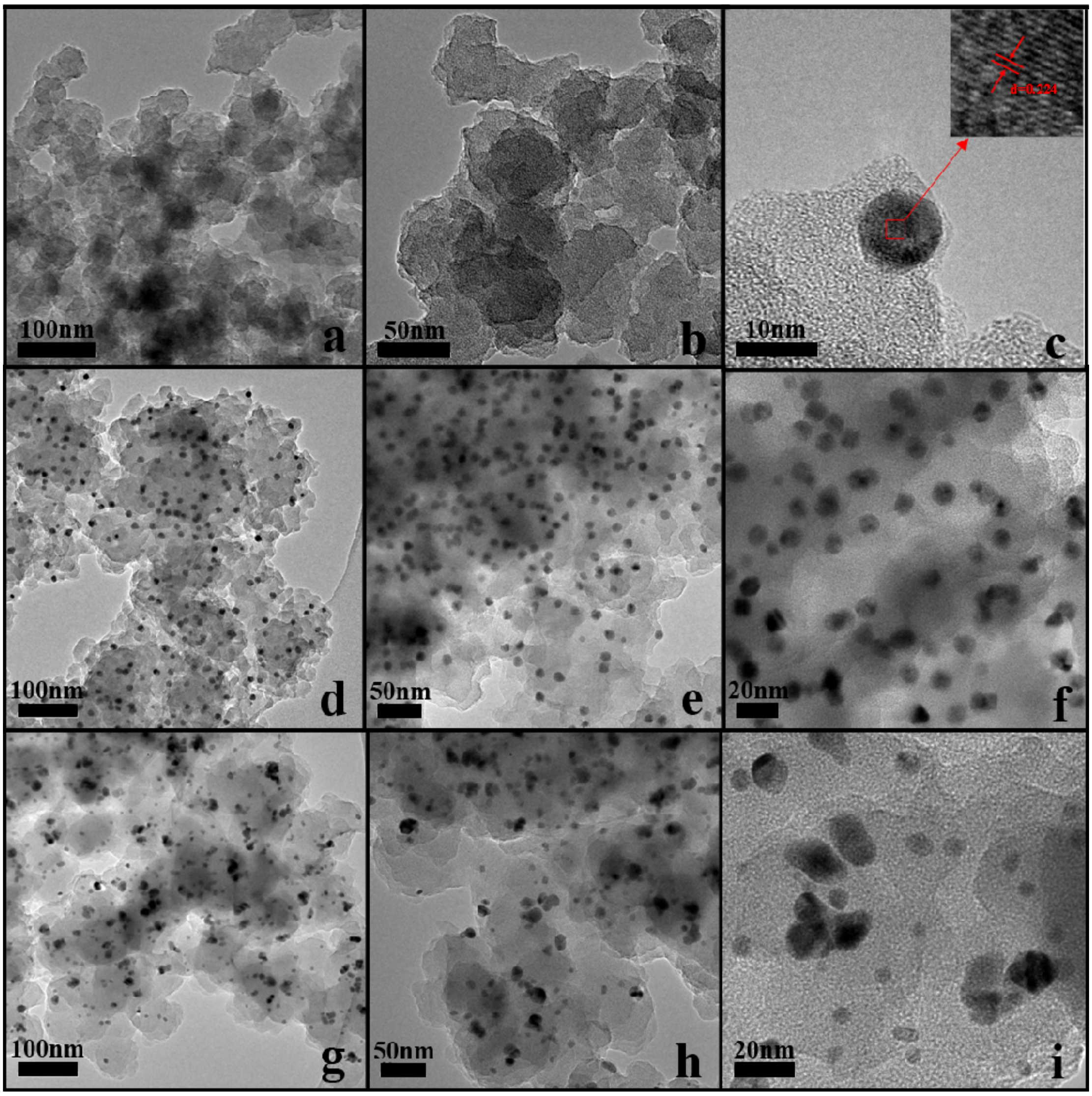

Figure S1. TEM images of COP-4 (a , b) ; Pd/COP-4-WH (c ,d, e, f); Pd/COP-4-DH (g, h, i).

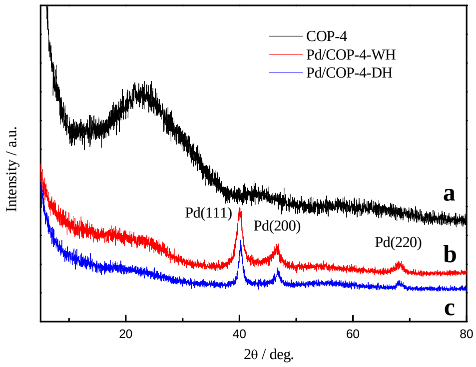

Figure S2. XRD patterns of (a) COP-4; (b) Pd/COP-4-WH; (c) Pd/COP-4-DH.

4. The isotherms and HK pore size distribution

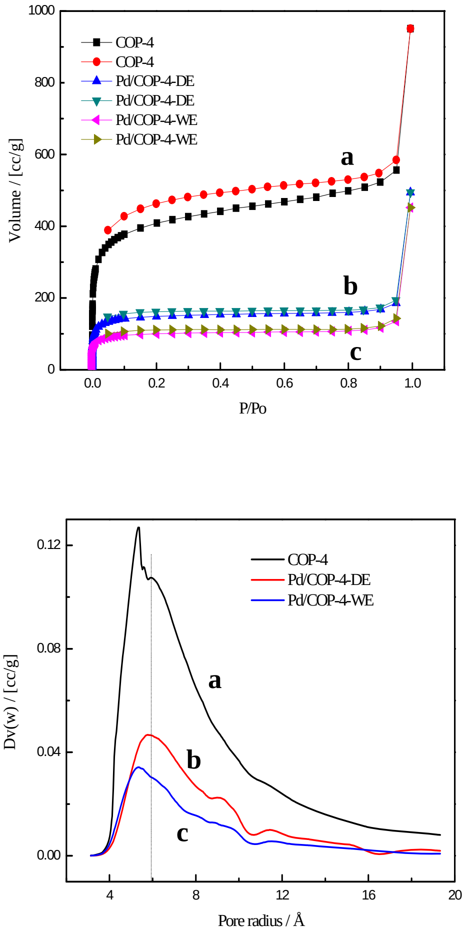

Figure S3. The isotherms (up) and HK pore size distribution (down) of (a) COP-4, (b) Pd/COP-4-DE, and (c) Pd/COP-4-WE.

5. TGA analysis

TGA was conducted to analyze the thermal stability of the samples. Before the analysis, all the samples were dried at 150 °C for 6 h in vacuum. The sample without electron reduction was also tested, which was dried at 60 °C for 12 h in vacuum and denoted as Pd/COP-4-D. As shown in Figure S4， no weight loss step could be found for COP-4 in inert gas up to 600 ^{o}C. Obviously, the electron reduction does not change the structure of COP-4. The weight loss of Pd/COP-4-D before 200 °C is more than 30%, indicating a large amount of DMF confined in the pores of COP-4. After drying at 150 °C for 6 h in vacuum, there is nearly no weight loss before 200 °C for all the samples. However, the two Pd/COP-4 samples have larger weight loss than COP-4 between 200 °C and 600 °C. From the DSC curves as well as the boiling point of DMF (152.8 °C), it is deduced that the weight loss before 200 °C is resulted from desorption of the residue solvent. The weight loss after 600 °C is mainly due to the decomposition of the COP-4 support, while the weight loss between 200 °C and 600 °C is caused by desorption of the solvent that has a strong interaction with the COP-4 support.

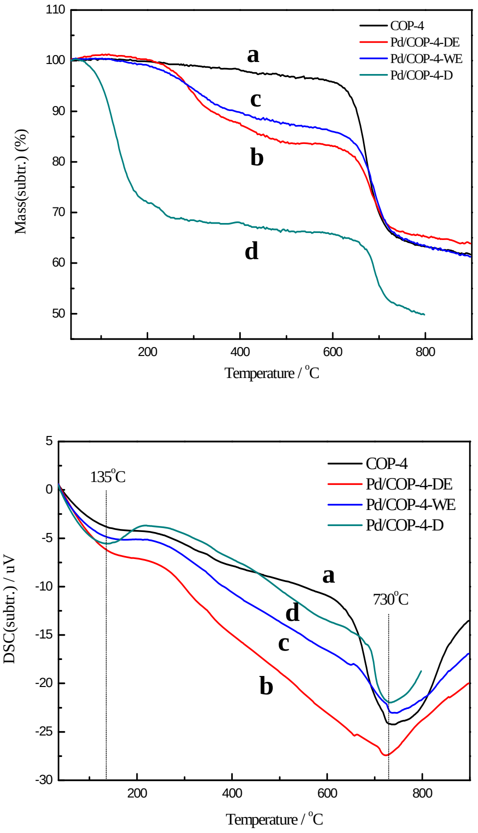

Figure S4. The TGA (up) and DSC (down) curves of (a) COP-4 (black), (b) Pd/COP-4-DE (red), (c) Pd/COP-4-WE (blue), and (d) Pd/COP-4-D (green).

6. TEM analyses of used catalysts

After reaction, the two Pd/COP-4 samples were characterized by TEM, as shown in Figure S5. The particle size of the two used catalysts increases slightly, compared to the fresh catalysts. The average sizes are 4.4 nm and 11.0 nm for the used Pd/COP-4-DE and the used Pd/COP-4-WE, respectively. This suggests that high temperature reaction results in an aggregation of the nano particles. We are performing other reactions in liquid phase at lower temperatures (from room temperature to 200 °C). We will confirm soon the properties of Pd/COP-4-DE and Pd/COP-4-WE in liquid reactions and will report them in our future publications.

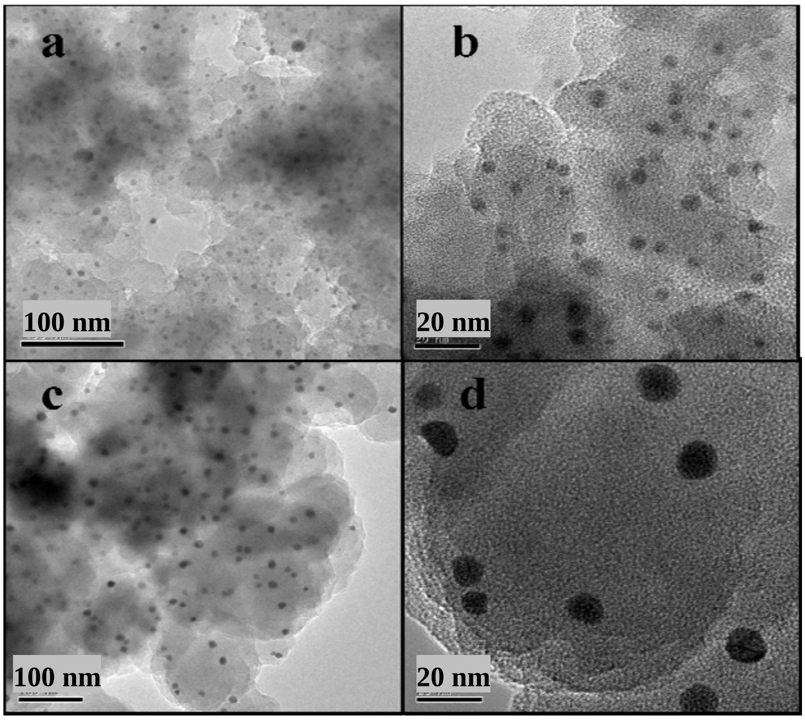

Figure S5. TEM images of the used Pd/COP-4-DE (a, b) and the used Pd/COP-4-WE (c, d)

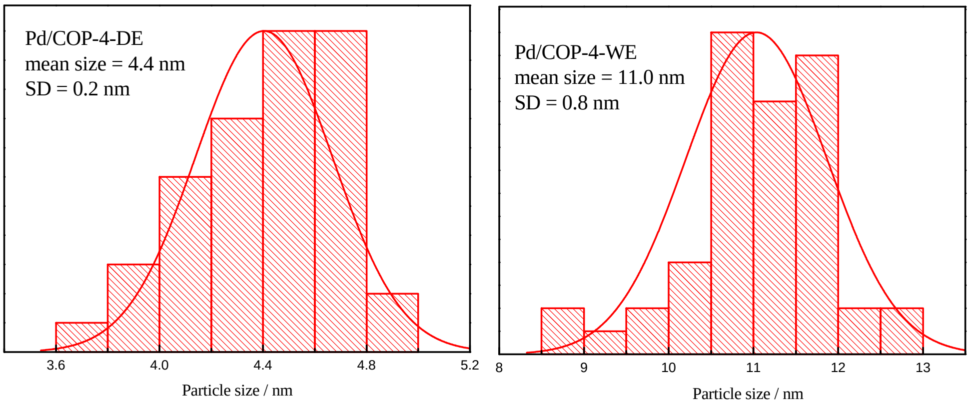

Figure S6. Particle size distributions of the used Pd/COP-4-DE (left) and the used Pd/COP-4-WE (right)